Conformal FDTD Simulation of Vibrating Intrinsic Reverberation Chambers

Florian Mahiddini, Guillaume Andrieu, Christophe Guiffaut, Nicolas Bui

Conformal FDTD Simulation of Vibrating Intrinsic Reverberation Chambers

Florian Mahiddini
XLIM, Université de Limoges
Limoges, France
florian.mahiddini@unilim.fr

Guillaume Andrieu
XLIM, Université de Limoges
Limoges, France
guillaume.andrieu@xlim.fr

Christophe Guiffaut
XLIM, CNRS
Limoges, France
christophe.guiffaut@xlim.fr

Nicolas Bui
XLIM, Université de Limoges
Limoges, France
nicolas.bui@xlim.fr

***Abstract*—We introduce a novel simulation procedure devoted to the inner field evaluation of arbitrary-shape reverberation chambers especially well-suited for the analysis of Vibrating Intrinsic Reverberation Chambers (VIRC). The described method is based on conformal Finite-Difference in Time-Domain (FDTD) modeling to account for the rough surface geometry of the VIRC walls. On this point, we took full advantage of the meshing capability of the in-house numerical code TEMSI developped by XLIM. Performance criteria typically introduced to evaluate the overall efficiency of conventional reverberation chambers (RC) are extracted from the computed S_{11} of a log-periodic antenna meshed within the under-study resonant cavity. Numerical outcomes demonstrate excellent agreement with experimental results in similar conditions.**

***Index Terms*—Conformal FDTD, FDTD, Reverberation chambers, VIRC, Well-Stirred condition method.**

I. Introduction

Reverberation chambers (RC) are electromagnetic cavity resonators commonly used by engineers and researchers to conduct a wide range of experiments including EMC tests, material characterization and over-the-air (OTA) testing of wireless devices. Conventional RC such as the one involved in EMC experiments are often heavy and costly apparatus whose performance extensively rely upon the design of an additional mode-stirrer. To overcome those drawbacks, a new kind of RC has been proposed in early 2000's, the so-called *Vibrating Intrinsic Reverberation Chamber* (VIRC). It consists in a cavity build as a tent made out of conductive fabric and whose vibrating movement ensure time-independent boundary conditions, thus avoiding the implementation of an heavy stirrer. Among the expected advantages of VIRC is the ability to conduct rapid and cost-effective experiments on large systems.

This article deals with the numerical modeling of a VIRC, which is a topic not particularly developed in the past. Indeed, although reverberation chambers have been widely studied throughout the years, surprisingly few communications have been made specifically about full-wave modeling of VIRC. In [1], authors emulated a set of 50 independent cavity models using a random surfaces creation algorithm as to take into account for the varying walls geometry over time. In their study, the reverberation conditions are assessed through the record of the electric field magnitude in the frequency domain of points located within the cavities along with a chi-squared Goodness-of-Fit test towards the Rayleigh distribution.
In [2], the authors proposed a somewhat similar procedure to both create random surfaces in FDTD and assess the field distribution. In their study, however, the authors dealt with the time-varying conditions of the walls by loading new surface geometries during the simulation which avoid running a consequent set of simulations.

Nevertheless, none of the aforementioned work has been able to reproduce wall configurations that match the realistic surfaces of a VIRC, as conventional FDTD methods solve Maxwell's equations on a given staircase mesh.

Furthermore, in these studies, the electric field is extracted from virtual points inside the cavities. This setup, although suitable from a numerical standpoint, does not easily permit a direct comparison with experimental data as it would require costly accessories such as electromagnetic field probes physically inserted in the reverberation chamber under test.

To enable such a comparison, the approach followed in this paper is the exact transposition of the recently introduced "well-stirred condition" method which relies on the sole determination of the S_{11}-parameter of an antenna [4], [5].

II. Principle of the Simulations

All the simulations described in this paper have been performed using the in-house FDTD code TEMSI developed at the XLIM laboratory. This software is able to handle a conformal mesh instead of a Cartesian grid as it is often the case with classical FDTD methods [6] . In addition to regular solving capability, TEMSI implements several interesting features helpful for VIRC characterization such as oblique thin wire modeling (implementing Holland formalism), conformal mesh and solver as well as OpenMP/MPI parallelization.

A. Walls surface generation

The generation of random surfaces is no new topic. The subject has been thoroughly investigated in computational electromagnetics, in particular to examine the field scattered

The present work is carried out within the framework of the project ASTRID/CHAOTIQ funded by DGA/AID and operated by the ANR, involving the laboratory XLIM, CISTEME and JDubois.

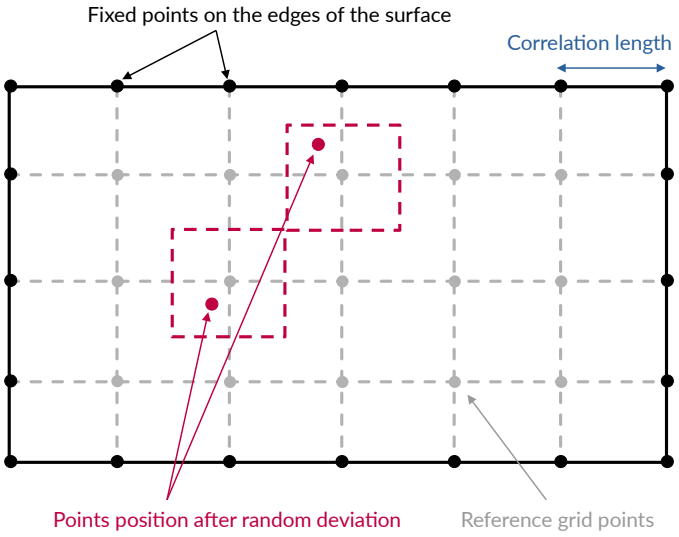

Fig. 1. Principles of random surfaces generation.

by sea surfaces (radar applications). In order to focus on the overall simulation procedure, and for the sake of simplicity, we chose to implement in this communication a very simple but yet efficient algorithm.

The procedure for generating wall surfaces is as follows. For each face of the VIRC, a reference grid is created with points spaced from each other with a distance corresponding to a desired *correlation length* C_L (sets to 10 cm in this paper). Except for the points on the edges of the surface, that are set to remain fixed, the new coordinates $X_i = (x(i); y(i); z(i))$ of the inner points are randomly computed using the following relations:

$$\begin{cases} x(i) &= x_g(i) + C_L k \left(\mathrm{r} - \dfrac{1}{2} \right) \\ y(i) &= y_g(i) + C_L k \left(\mathrm{r} - \dfrac{1}{2} \right) \\ z(i) &= z_g(i) + C_L k \left(\mathrm{r} - \dfrac{1}{2} \right) \end{cases} \quad \text{with } 0 \leqslant k \leqslant 1 \quad (1)$$

where $X_g = (x_g(i); y_g(i); z_g(i))$ are the points coordinates of the reference grid, k is an empirical coefficient related to the authorized movement of each point and r a random number included in the range between 0 and 1.

For every generated mesh (which corresponds to the geometry of the VIRC at a given instant), a Matlab program computes the coordinates of each point and exports these information in a STL format file. Each square area shown in Fig. 1 are discretized into two triangles along one of its diagonal. The STL file is finally made ready for simulation by our in-house conformal FDTD mesher.

B. Loss Insertion

The VIRC walls are modeled as perfect electric conductors (PEC). In order to account for the cavity losses, we have implemented a specific post-processing operation which consists in applying an exponential filter on the inner field recorded inside the cavity (Fig. 2). This method is described in [7] and has been proven experimentally relevant for reverberation chamber characterization in [8]. With this approach, the losses are linked to the exponential decay S via the following relations:

$$S = \exp\left(\frac{-\pi f_0 t}{Q}\right) = \exp\left(-\pi \Delta f t\right) \quad (2)$$

where Q stands for the quality factor of the VIRC and Δf the average mode bandwidth at a given frequency f_0 defined as the ratio $Q(f_0)/f_0$ (assumed to be frequency independent here).

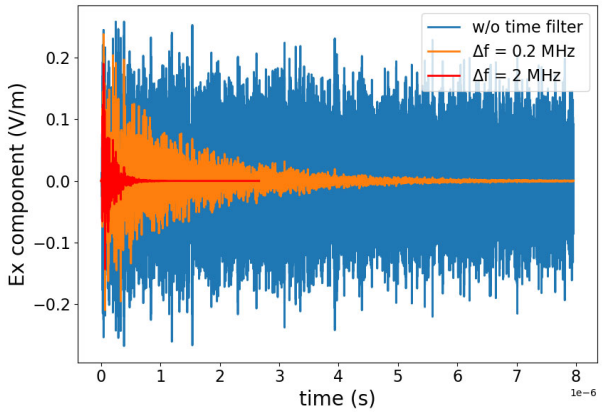

Fig. 2. Exponential time-filtering for two Δf values.

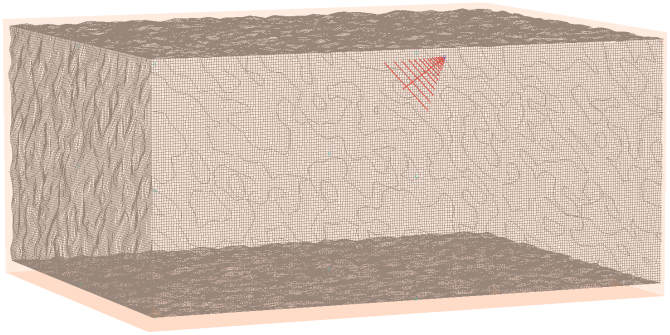

Fig. 3. Conformal mesh visualization of one geometry of the simulated VIRC.

III. Results

A. Description of the VIRC under test

A batch of 50 VIRC models, with dimensions $4.5 \times 3.5 \times 2$m, have been meshed following the procedure described in the previous sections. Those 50 configurations are uncorrelated by construction. An example of one such geometry processed by the TEMSI's conformal mesh generator is shown in Fig. 3.

The maximum frequency of the study is given by the dimension of the regular FDTD mesh size, which has been here set to 2 cm. Considering the common stability criteria $\lambda_{\max}/10$, it implies a maximum frequency of $f_{\max} = 1.5$ GHz. The number of cells is $239 \times 189 \times 114$ with respect to the three Cartesian directions.

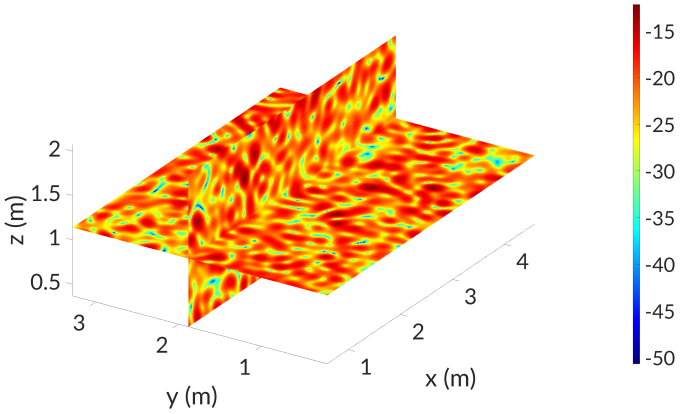

Fig. 4. 3D map E-field amplitude. Results expressed in dBV/m ($t = 5.6 \times 10^{-6}$ s).

The emitting antenna is a log-periodic antenna build with a collection of oblique thin wires [9] and designed to radiate over a bandwidth between 0.3 and 1.5 GHz. The antenna is located in one of the upper corner of the VIRC, at a distance greater than $\lambda_{\text{min}}/2$ of the walls as depicted in Fig. 3. The antenna excitation is achieved by a Gaussian impulse (combined with a sine wave modulation) voltage source of central frequency 900 MHz.

The computations of the 50 configurations were performed on the HPC cluster CALI provided by the University of Limoges. At least 15 simulations were able to run on parallel, each one of them being distributed on 4 processors, for an estimated computation time of about 12 hours per simulation.

B. Preliminary results

We are first showing a 3D mapping of the total electric field obtained in the VIRC for an average mode bandwidth of Δf = 0.2 MHz in Fig. 4. It is clear that this mapping corresponds to the case of a diffuse field.

C. The "Well-Stirred Condition" Method

The "Well-Stirred Condition" method aims at defining the minimum frequency called f_{wsc} from which an RC can be considered as *well-stirred*. According to the definition of this condition given in [4], the electromagnetic (EM) field distributions and the sample correlation (through the first-order autocorrelation coefficient $r(1)$ analysis) have to be assessed. This method has been applied on VIRC experimental results in [3]. It has been shown that, when the delay between two measurements is large, the correlation is null (i.e. the movement of the tent has been sufficient to obtain a new independent geometry of the VIRC) and therefore the key result is the analysis of the EM field distributions through the Anderson-Darling goodness-of-fit (AD GOF) test.

D. Results

The S_{11} magnitude of the antenna calculated on the bandwidth 0.2 to 1.5 GHz is given in Fig. 5 for each generated geometry and for two different values of the average mode bandwidth Δf (i.e. 0.2 and 1 MHz). As expected, the S_{11} parameter is heavily affected by the quality factor of the cavity. In addition, the S_{11} parameter calculated in free space is added for comparison. It is particularly clear that the presented results looks like experimental results, for instance the ones obtained in [3].

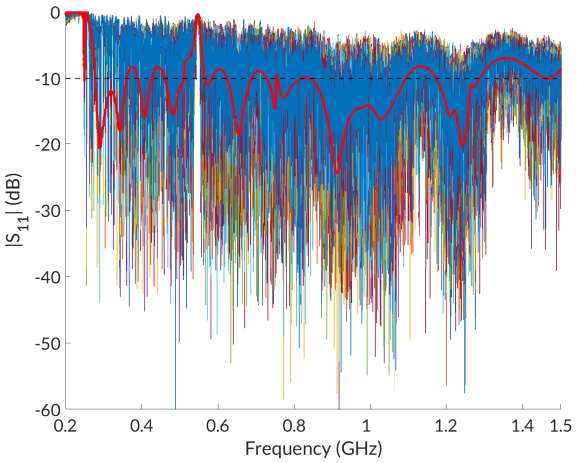

(a) Obtained results for $\Delta f = 0.2$ MHz

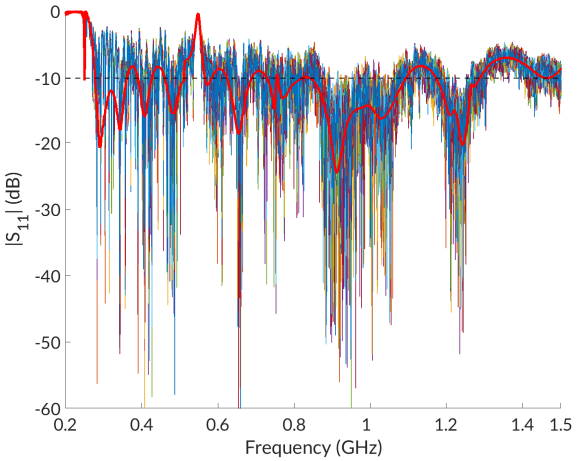

(b) Obtained results for $\Delta f = 1$ MHz

Fig. 5. Magnitude of the S_{11} parameter (in red, the same result obtained in free space).

The frequency dependence of the AD GOF test as well as the first-order autocorrelation coefficient are presented for the same values of the average mode bandwidth in Fig. 6.

We can notice that the different geometries of the VIRC lead to uncorrelated results even at 200 MHz. Moreover, the Rayleigh distribution is matched at a lower frequency when Δf increases, in total agreement with results already published in the literature, for instance in [3], [4], [8].

All the frequencies f_{wsc} (which are here equal to f_1) from which the RC can be considered as "well-stirred" obtained

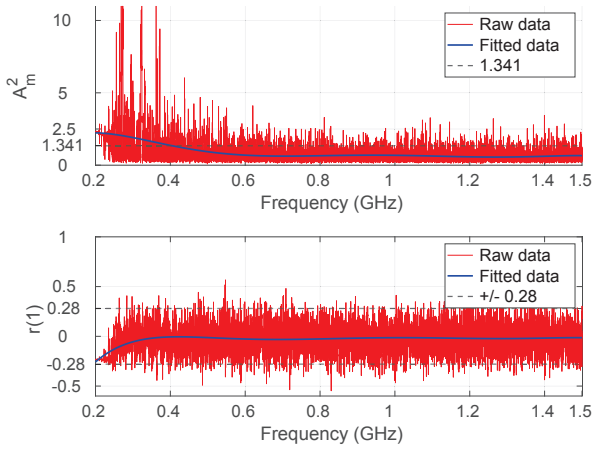

(a) $\Delta f = 0.2$ MHz

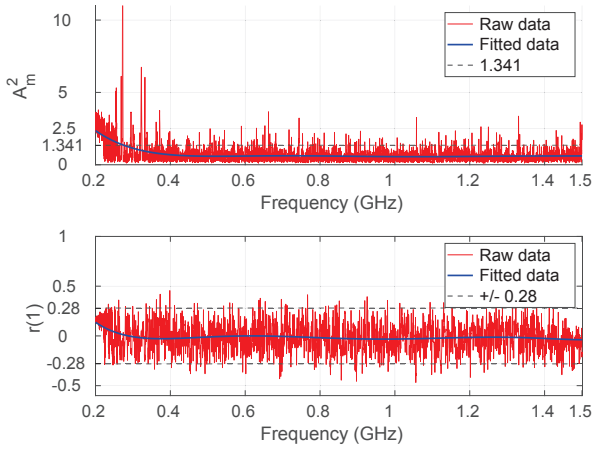

(b) $\Delta f = 1$ MHz

Fig. 6. Anderson-Darling GoF and first-order autocorrelation coefficients (and their polynomial curve fit) obtained for both values of the average mode bandwidth Δf. Comparison with the threshold values of respectively 1.341 and 0.28.

for different values of Δf are listed in Table 1. It is clear that f_1 severely decreases when Δf increases, an effect which is similar to the insertion of a block of absorbers within an RC.

IV. Conclusion and Perspectives

This paper has presented for the first time electromagnetic simulations of a VIRC using a conformal FDTD method. The results are particularly promising as they confirm experimental results previously obtained at XLIM. In the near future, we first plan to study different processes in order to reproduce as much as possible the realistic surface of a VIRC tent. Secondly, we will try to introduce correlation between two successive geometries in order to reproduce the effect of a proper VIRC movement.

TABLE I
Results obtained by the "well-stirred" condition method for different average mode bandwidth values

Δf (MHz)	Q @ 1 GHz	τ (s)	f_{wsc} (MHz)
0.2	7500	1.59E-06	405.4
0.3	5000	1.06E-06	374.4
0.4	3750	7.96E-07	360.4
0.5	3000	6.37E-07	334.8
0.6	2500	5.31E-07	303.2
0.8	1875	3.98E-07	297.2
1.0	1500	3.18E-07	276.5
1.2	1250	2.65E-07	<200
1.4	1071	2.27E-07	<200
1.6	937	1.99E-07	<200
1.8	833	1.77E-07	<200
2.0	750	1.59E-07	<200

References

[1] M. Hara, Y. Takahashi, R. Vogt-Ardatjew and F. Leferink, "Validation of Vibrating Intrinsic Reverberation Chamber using Computational Electromagnetics," 2019 Joint International Symposium on Electromagnetic Compatibility, Sapporo and Asia-Pacific International Symposium on Electromagnetic Compatibility (EMC Sapporo/APEMC), 2019, pp. 593-596, doi: 10.23919/EMCTokyo.2019.8893677.

[2] N. K. Kouveliotis, P. T. Trakadas, and C. N. Capsalis, "FDTD modeling of Vibrating Intrinsic Reverberation Chambers", Progress In Electromagnetics Research, PIER 39, 47–59, 2003

[3] G. Andrieu, N. Meddeb, C. Jullien and N. Ticaud, "Complete Framework for Frequency and Time-Domain Performance Assessment of Vibrating Intrinsic Reverberation Chambers," in IEEE Transactions on Electromagnetic Compatibility, vol. 62, no. 5, pp. 1911-1920, Oct. 2020, doi: 10.1109/TEMC.2020.2966741.

[4] G. Andrieu, N. Ticaud, F. Lescoat and L. Trougnou, "Fast and Accurate Assessment of the "Well Stirred Condition" of a Reverberation Chamber From S_{11} Measurements," in IEEE Transactions on Electromagnetic Compatibility, vol. 61, no. 4, pp. 974-982, Aug. 2019, doi: 10.1109/TEMC.2018.2847727.

[5] G. Andrieu, "Electromagnetic Reverberation Chambers : Recent advances and innovative applications", IET, Dec. 2020.

[6] N. Bui, C. Guiffaut and A. Reineix, "Field interpolation with generalized barycentric coordinates in conformal FDTD schemes," 2019 IEEE International Symposium on Antennas and Propagation and USNC-URSI Radio Science Meeting, 2019, pp. 1651-1652.

[7] G. Orjubin, F. Petit, E. Richalot, S. Mengue and O. Picon, "Cavity losses modeling using lossless FDTD method," in IEEE Transactions on Electromagnetic Compatibility, vol. 48, no. 2, pp. 429-431, May 2006, doi: 10.1109/TEMC.2006.873854.

[8] A. Adardour, G. Andrieu and A. Reineix, "On the Low-Frequency Optimization of Reverberation Chambers," in IEEE Transactions on Electromagnetic Compatibility, vol. 56, no. 2, pp. 266-275, April 2014, doi: 10.1109/TEMC.2013.2288001.

[9] C. Guiffaut, A. Reineix and B. Pecqueux, "New Oblique Thin Wire Formalism in the FDTD Method With Multiwire Junctions," in IEEE Transactions on Antennas and Propagation, vol. 60, no. 3, pp. 1458-1466, March 2012.